Simulation of a neuroimaging acquisition with MAPSSIC, an implantable β^+ microprobe for rat brain imaging

S. El ketara[a,b], F. Agnese[d], L. Ammour[c], J. Baudot[d], S. Bouvard[e], O. Clausse[d], M. Dupont[f], F. Gensolen[f], M. Goffe[d], M. Kachel[d], J. Laurence[f], T. Weicherding[f], C. Wabnitz[d], C. Morel[f], P. Pangaud[f], L. Zimmer[d], P. Lanièce[a,b], M.-A. Verdier[a,b]

[a]Université Paris-Saclay, CNRS/IN2P3, IJCLab, 91405 Orsay, France

[b]Université Paris Cité, IJCLab, 91405 Orsay France

[c]Nantes Université, CHU Nantes, F-44000 Nantes, France

[d]Université de Strasbourg, CNRS, IPHC UMR 7178, F-67000 Strasbourg, France

[e]Université Claude Bernard Lyon 1, CERMEP-Imagerie du vivant, CNRS, INSERM, Hospices Civils de Lyon, Lyon, France

[f]Aix Marseille Univ, CNRS/IN2P3, CPPM, Marseille, France

Preclinical neuroimaging with micro-PET

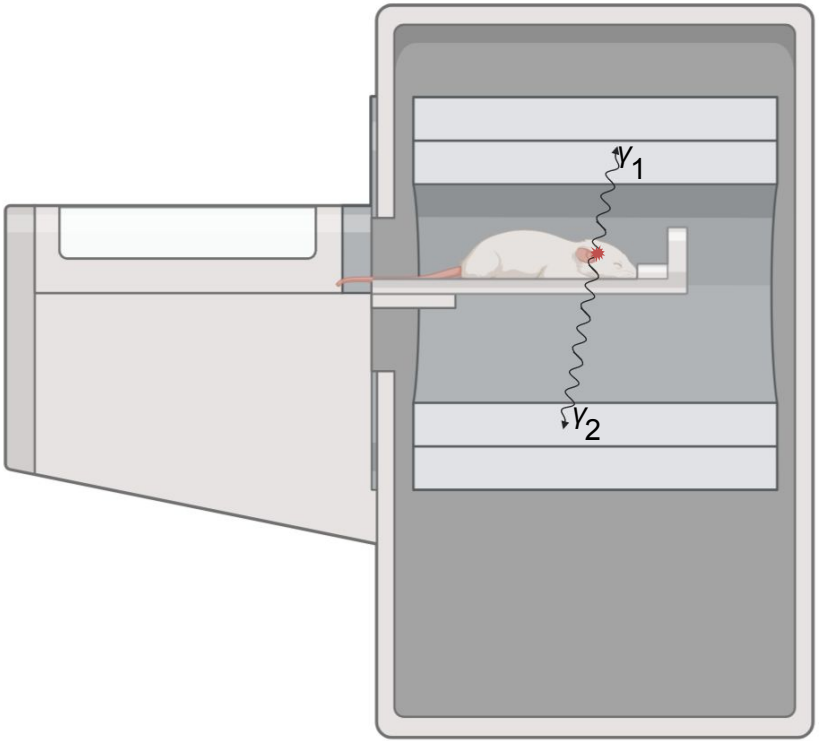

micro-**Positron Emission Tomography** (micro-PET):

- Use injected β^+ radioisotopes
- Detects gamma rays from β^+/e- annihilation
- **High sensitivity**
- Allows for **quantification**

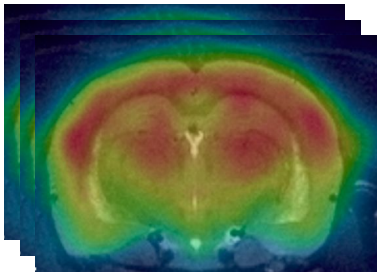

Preclinical neuroimaging with micro-PET

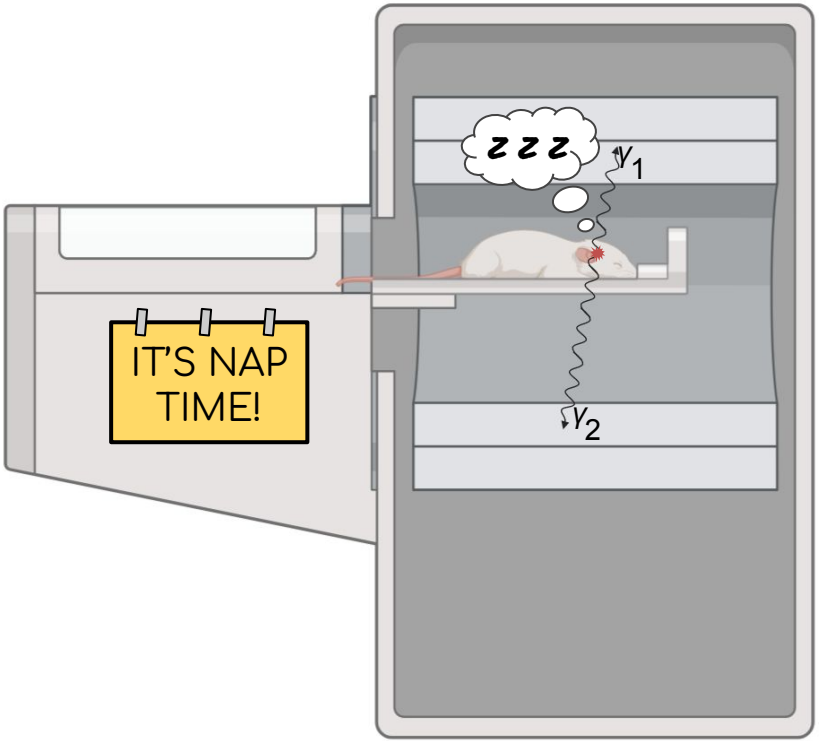

micro-**Positron Emission Tomography** (micro-PET):

- Use injected β^+ radioisotopes
- Detects gamma rays from β^+/e- annihilation
- **High sensitivity**
- Allows for **quantification**
- **Requires anesthesia**

→ Need for **awake imaging** data

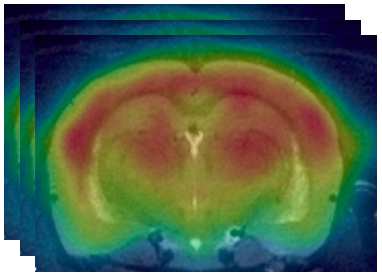

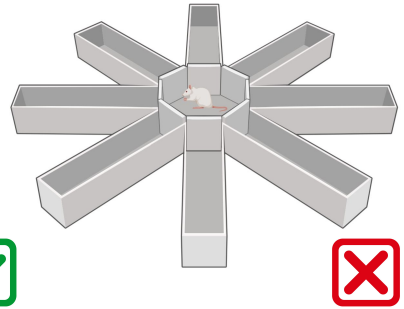

Neuroimaging of awake and freely moving rats, why?[1]

Majority of preclinical imaging performed under anesthesia

[1] *Y.R. Gao et al, NeuroImage, 2017*
[2] *J. Silverman, Laboratory animal science*

Neuroimaging of awake and freely moving rats, why?[1]

Majority of preclinical imaging performed under anesthesia

Effect of anesthesia

→ Potential biases
→ Many anesthetics[2]

[1] *Y.R. Gao et al, NeuroImage, 2017*
[2] *J. Silverman, Laboratory animal science*

Neuroimaging of awake and freely moving rats, why?[1]

Majority of preclinical imaging performed under anesthesia

Effect of anesthesia

→ Potential biases
→ Many anesthetics[2]

Get closer to clinical practices

→ No anesthesia in clinical imaging

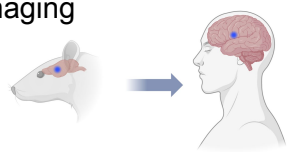

[1] *Y.R. Gao et al, NeuroImage, 2017*
[2] *J. Silverman, Laboratory animal science*

Neuroimaging of awake and freely moving rats, why?[1]

Majority of preclinical imaging performed under anesthesia

Effect of anesthesia

→ Potential biases
→ Many anesthetics[2]

Get closer to clinical practices

→ No anesthesia in clinical imaging

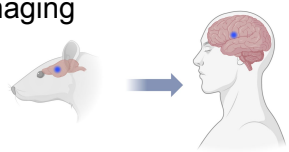

Perform **simultaneous neuroimaging** and **behaviour** studies

→ Correlation between behavior and brain images
→ Molecular processes allow better understanding of behavior

Effort made for **all modalities** (MRI, ultrasound and optic imaging)

[1] *Y.R. Gao et al, NeuroImage, 2017*
[2] *J. Silverman, Laboratory animal science*

Neuroimaging on awake and freely moving rats: 3 approaches

1 mini microPET

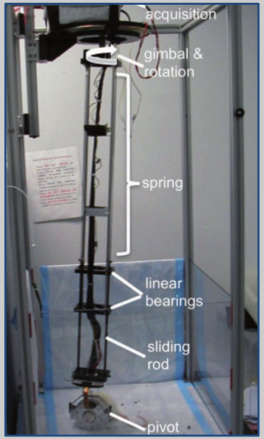

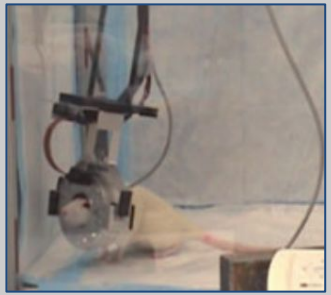

Schulz et al., Nature methods, 2011.

2 Regular microPET with Motion tracking

Spangler-Bickell et al., Phys. Med. Biol., 2016.

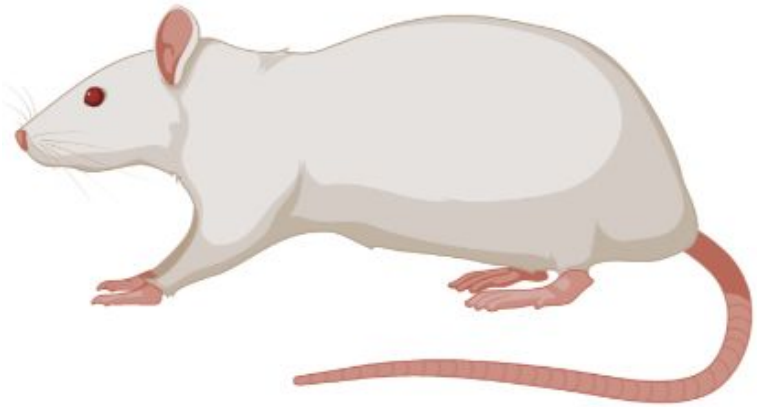

3 Implantable Microprobe

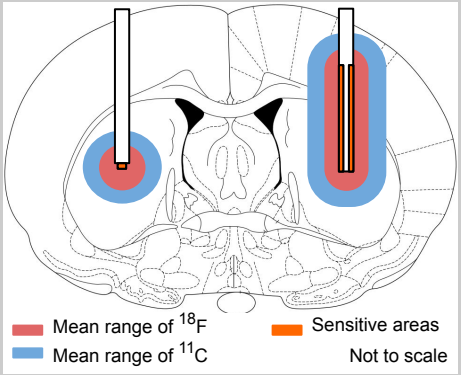

Pain et al., PNAS, 2002.

L. Balasse et al., Mol Imaging Biol, 2015

Neuroimaging on awake and freely moving rats: 3 approaches

1 mini microPET

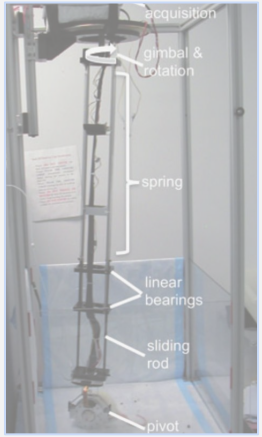

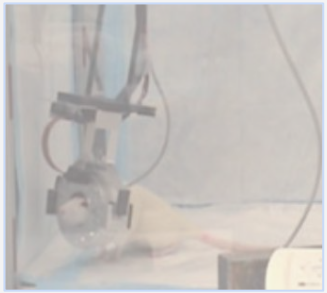

Schulz et al., Nature methods, 2011.

2 Regular microPET with Motion tracking

Spangler-Bickell et al., Phys. Med. Biol., 2016.

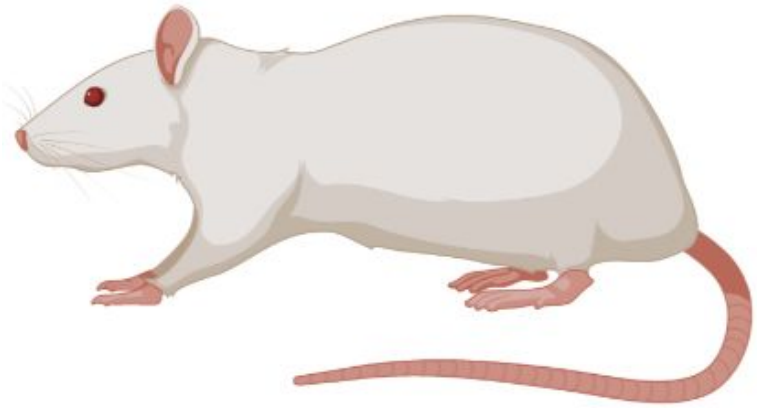

3 Implantable Microprobe

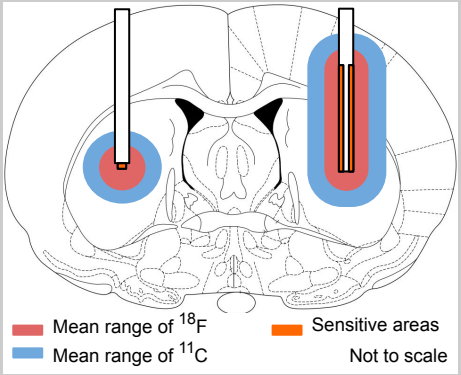

Pain et al., PNAS, 2002.

L. Balasse et al., Mol Imaging Biol, 2015

MAPSSIC project

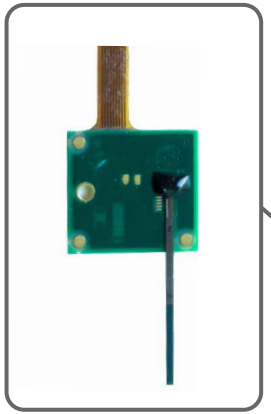

1. Implantable probe

2. Backpack
- Microcontroller
- Power supply
- RF antenna

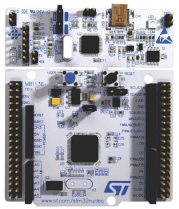

Microcontroller STM32

CR1/3N Lithium Battery

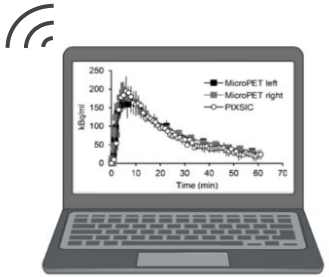

Features:
- Sensitive to **short range β⁺**
- Record **kinetic** of **radiotracers**
- **Autonomy** to the rat
  ⟶ **Wireless**

Constraints:
- **Gamma transparency**
- **Light:** < 10% of rat weight
- **Biocompatible**
- **Low power consumption**

MAPSSIC project

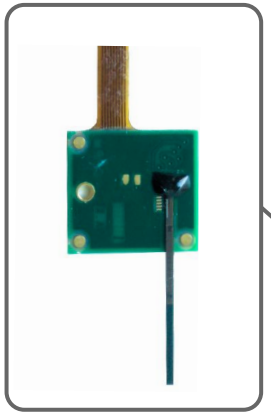

1. Implantable probe

2. Backpack
- Microcontroller
- Power supply
- RF antenna

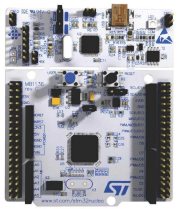

Microcontroller STM32

CR1/3N Lithium Battery

2022 → Sensor Production

2023 → Characterization/ MC studies

2024 → Biological validation

2025 → Behavioural applications

Features:
- Sensitive to **short range β⁺**
- Record **kinetic** of **radiotracers**
- **Autonomy** to the rat
  ⟶ **Wireless**

Constraints:
- **Gamma transparency**
- **Light:** < 10% of rat weight
- **Biocompatible**
- **Low power consumption**

MAPSSIC probe

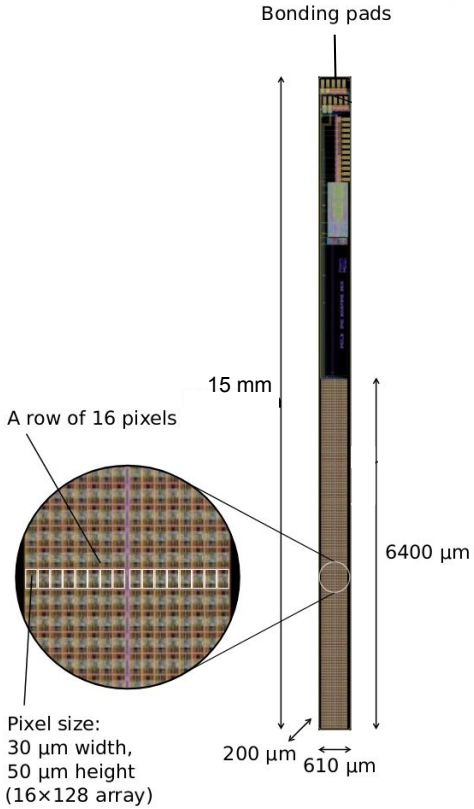

New digital sensor prototype (**IMIC**, 2022) based on a first prototype[1,2] (2018):

- Based on **CMOS-MAPS technology**
- Totale / Sensitive thickness: 200 µm / **25-50 µm**
- Pixel digitation: **1 bit**
- **Rolling shutter** readout

[1] *L. Amour et al., IEEE Transactions on Radiation and Plasma Medical Sciences, 2019*
[2] *J. Heymes et al., IEEE Nuclear Science Symposium, Medical Imaging Conference, 2016*

MAPSSIC probe

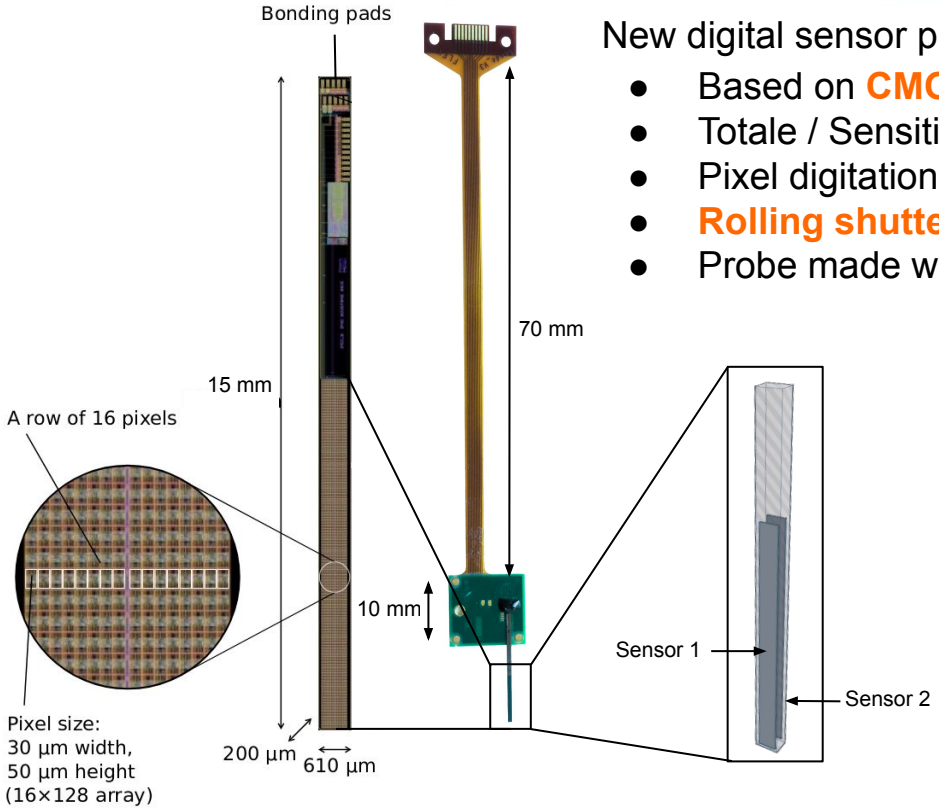

New digital sensor prototype (**IMIC**, 2022) based on a first prototype[1,2] (2018):

- Based on **CMOS-MAPS technology**
- Totale / Sensitive thickness: 200 µm / **25-50 µm**
- Pixel digitation: **1 bit**
- **Rolling shutter** readout
- Probe made with **2 sensors** glued back-to-back

[1] *L. Amour et al., IEEE Transactions on Radiation and Plasma Medical Sciences, 2019*
[2] *J. Heymes et al., IEEE Nuclear Science Symposium, Medical Imaging Conference, 2016*

MAPSSIC probe

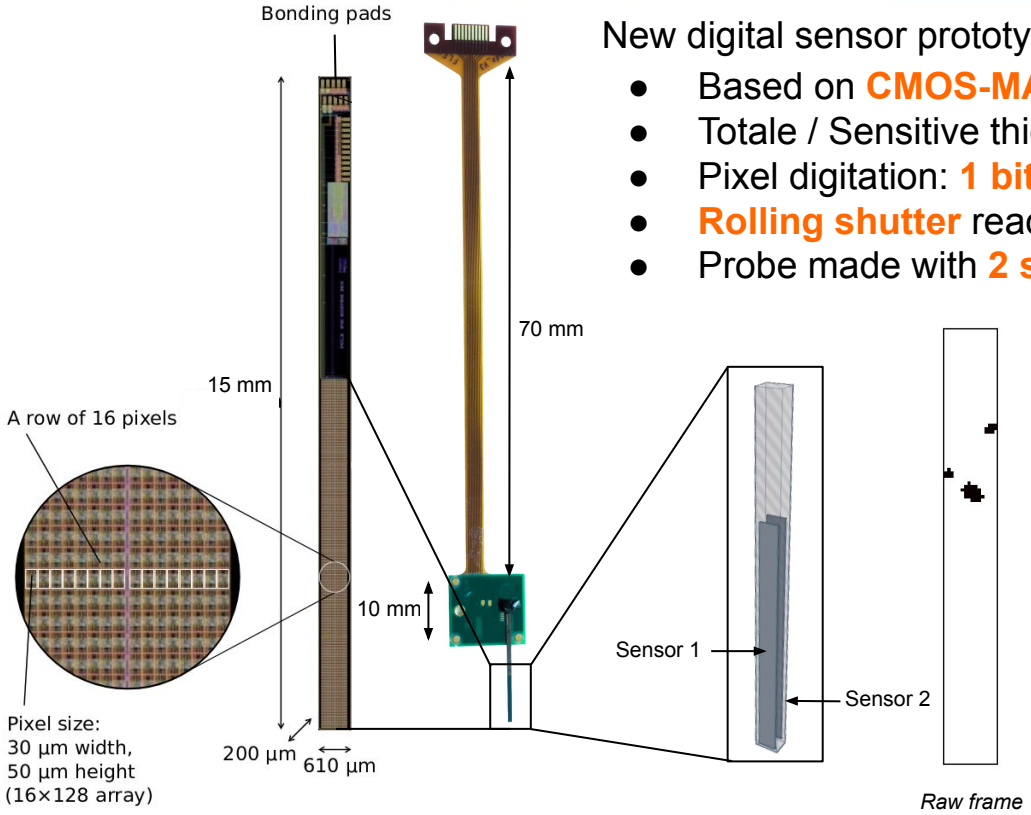

New digital sensor prototype (**IMIC**, 2022) based on a first prototype[1,2] (2018):

- Based on **CMOS-MAPS technology**
- Totale / Sensitive thickness: 200 µm / **25-50 µm**
- Pixel digitation: **1 bit**
- **Rolling shutter** readout
- Probe made with **2 sensors** glued back-to-back

[1] *L. Amour et al., IEEE Transactions on Radiation and Plasma Medical Sciences, 2019*
[2] *J. Heymes et al., IEEE Nuclear Science Symposium, Medical Imaging Conference, 2016*

MAPSSIC probe

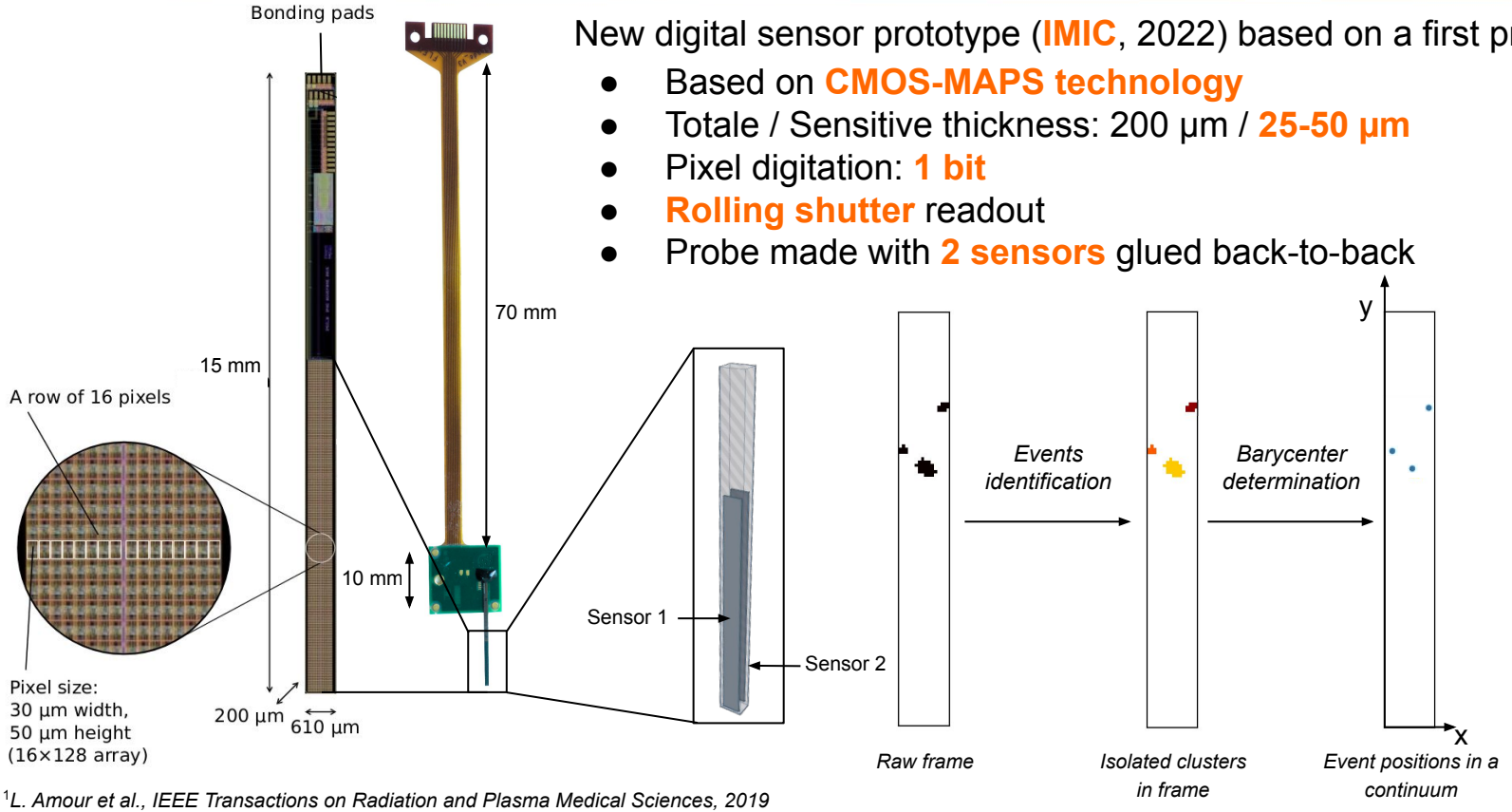

New digital sensor prototype (**IMIC**, 2022) based on a first prototype[1,2] (2018):

- Based on **CMOS-MAPS technology**
- Totale / Sensitive thickness: 200 µm / **25-50 µm**
- Pixel digitation: **1 bit**
- **Rolling shutter** readout
- Probe made with **2 sensors** glued back-to-back

[1] *L. Amour et al., IEEE Transactions on Radiation and Plasma Medical Sciences, 2019*
[2] *J. Heymes et al., IEEE Nuclear Science Symposium, Medical Imaging Conference, 2016*

MAPSSIC probe

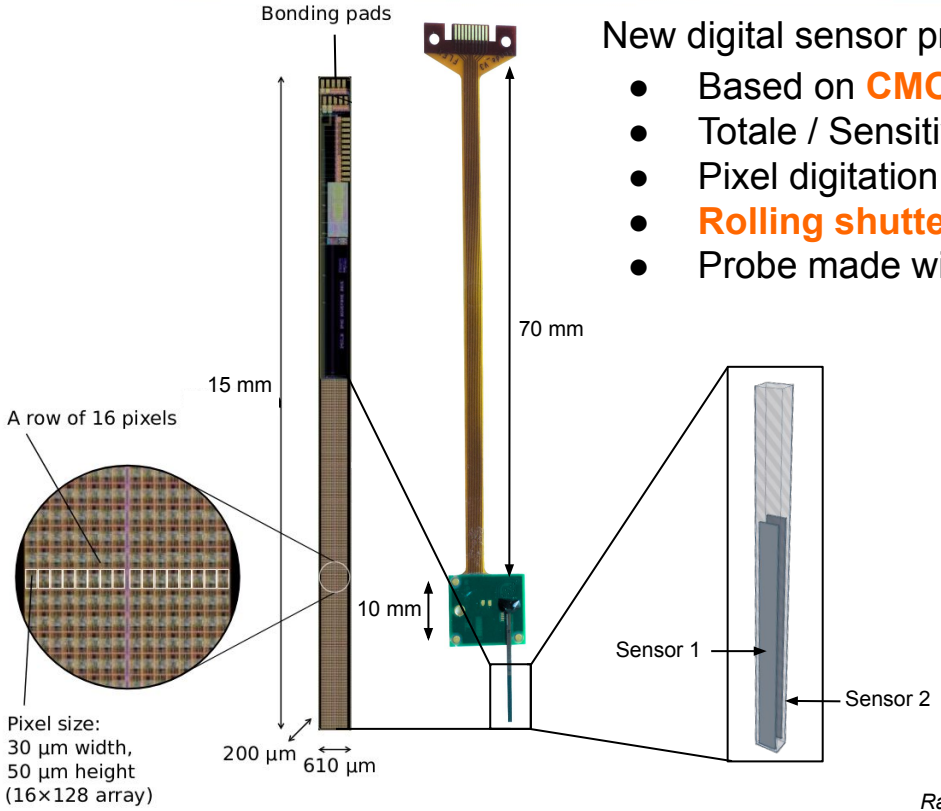

New digital sensor prototype (**IMIC**, 2022) based on a first prototype[1,2] (2018):

- Based on **CMOS-MAPS technology**
- Totale / Sensitive thickness: 200 µm / **25-50 µm**
- Pixel digitation: **1 bit**
- **Rolling shutter** readout
- Probe made with **2 sensors** glued back-to-back

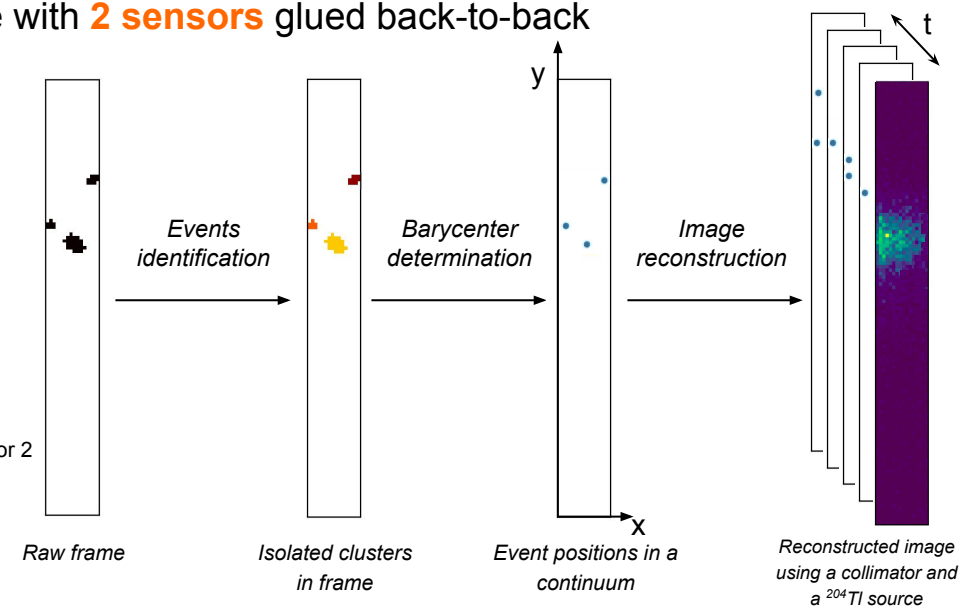

[1] *L. Amour et al., IEEE Transactions on Radiation and Plasma Medical Sciences, 2019*
[2] *J. Heymes et al., IEEE Nuclear Science Symposium, Medical Imaging Conference, 2016*

MAPSSIC overview

Probe mounting

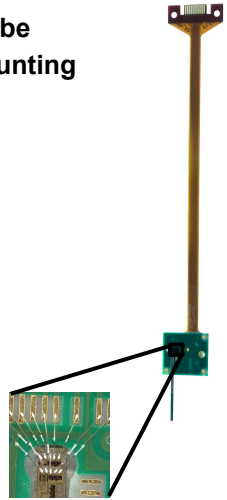

Wire connections

Back-to-back sensor assembling

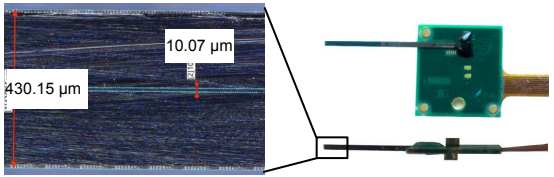

MAPSSIC overview

Probe mounting

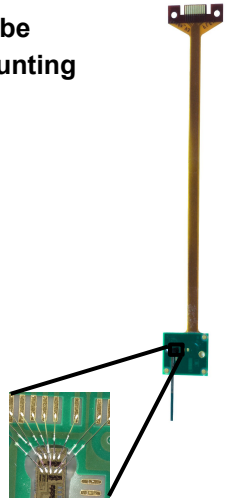

Wire connections

Biology

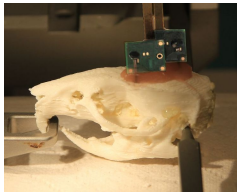

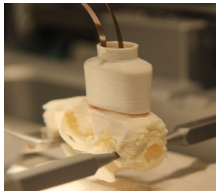

3D printed rat skull

Back-to-back sensor assembling

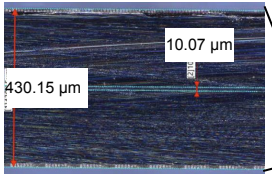

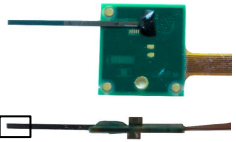

MAPSSIC overview

Probe mounting

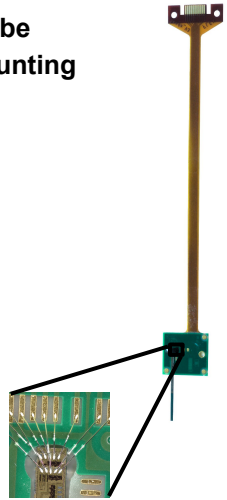

Wire connections

Biology

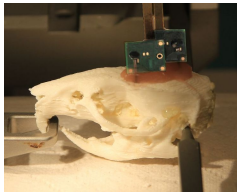

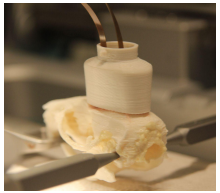

3D printed rat skull

Electronics

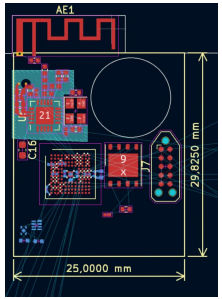

Microcontroller scheme

Back-to-back sensor assembling

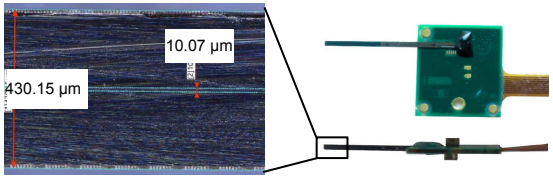

MAPSSIC overview

Probe mounting

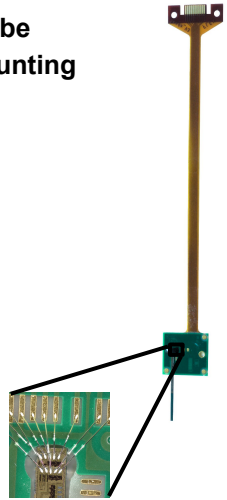

Wire connections

Biology

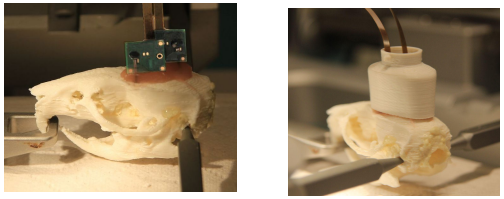

3D printed rat skull

Electronics

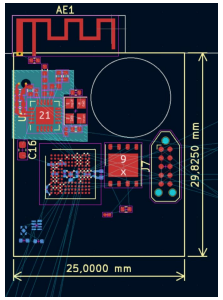

Microcontroller scheme

Back-to-back sensor assembling

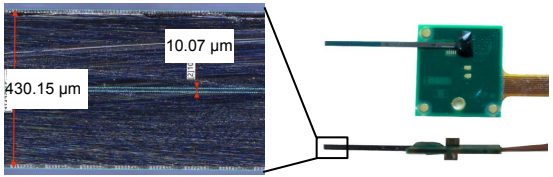

Clustering analysis

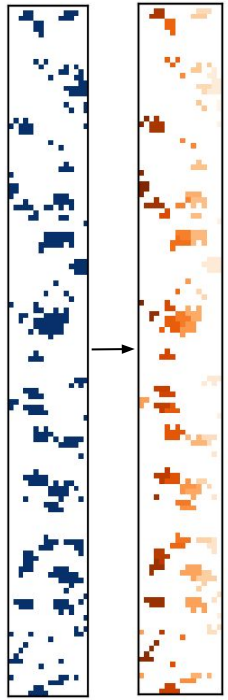

Machine learning method for event reconstruction

MAPSSIC overview

Physical validation and sensor optimisation

Testing PCB

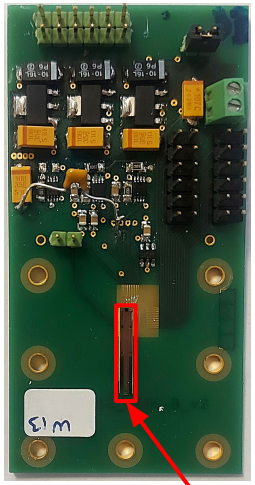

IMIC sensor

→ Energy threshold

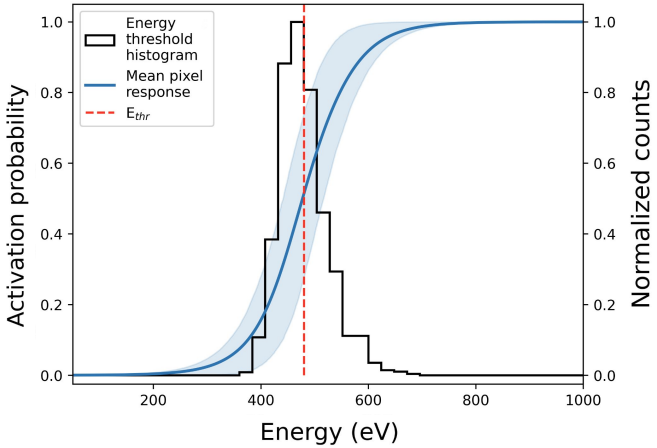

Understand the sensor's characteristics

Set nominal parameters

- **Charge injections**
- **Sealed sources**
  - beta: ^{204}Tl, ^{22}Na
  - X ray: ^{55}Fe

MAPSSIC overview

Physical validation and sensor optimisation

Testing PCB

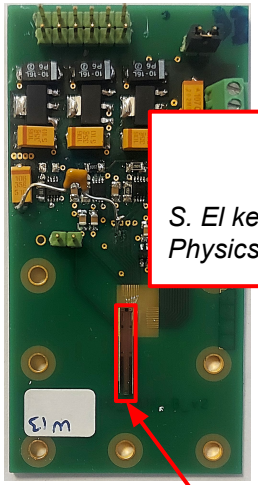

IMIC sensor

→ Energy threshold

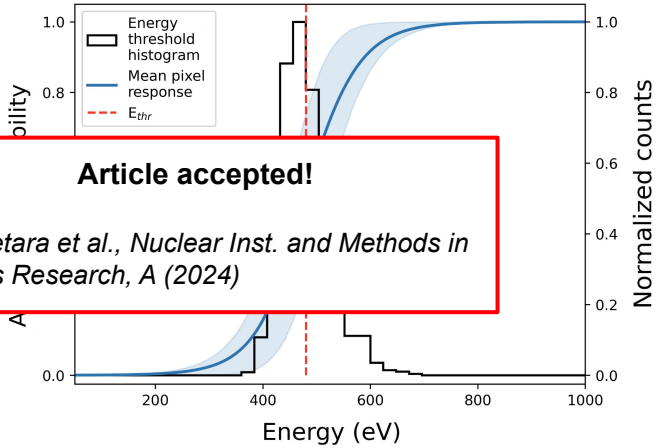

Article accepted!

S. El ketara et al., Nuclear Inst. and Methods in Physics Research, A (2024)

Understand the sensor's characteristics

Set nominal parameters

- **Charge injections**
- **Sealed sources**
  - beta: ^{204}Tl, ^{22}Na
  - X ray: ^{55}Fe

MAPSSIC overview

Physical validation and sensor optimisation

Testing PCB

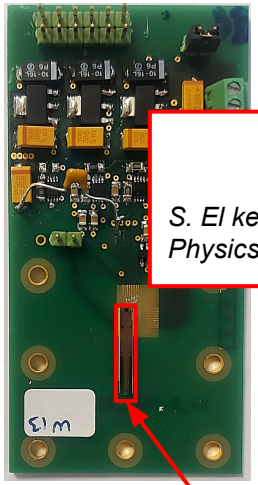

IMIC sensor

→ Energy threshold

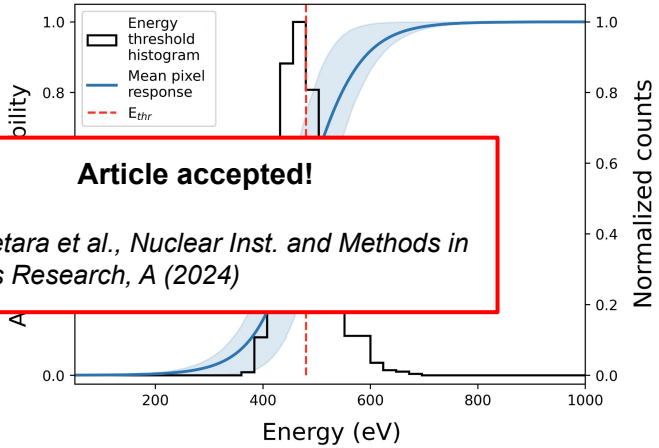

Article accepted!

S. El ketara et al., Nuclear Inst. and Methods in Physics Research, A (2024)

Understand the sensor's characteristics

Set nominal parameters

- **Charge injections**
- **Sealed sources**
  - beta: ^{204}Tl, ^{22}Na
  - X ray: ^{55}Fe

Simulations of an in vivo experiment

- Confirm the probe relevance
- Predict its *in vivo* performances
- Explore segmentation methods

→ **Monte Carlo simulations using GATE**

Input - Geometry

ROBY phantom[1]

Voxelized rat phantom:

- Generated with the **ROBY program**[1]
  - Skull area: cubic voxels of 100 µm sides
  - Body area: cubic voxels of 1 mm sides
- Used for both **attenuation** and **activity** ranges
- Addition of **Harderian glands** from MRI images

[1] *W. P. Segars, Molecular Imaging and Biology, 2004.*

Input - Geometry

ROBY phantom[1]

Voxelized rat phantom:

- Generated with the **ROBY program**[1]
  - Skull area: cubic voxels of 100 µm sides
  - Body area: cubic voxels of 1 mm sides
- Used for both **attenuation** and **activity** ranges
- Addition of **Harderian glands** from MRI images

Probes geometry:

- **2 Silicon boxes** of 9500 µm x 450 µm x 700 µm
- Physical volume inserted within the voxelized phantom using the **Merge Volume Actor**
- In the **cerebellum** and **striatum** region
- **Sensitive areas** of 6400 µm x 25 (and 50) µm x 480 µm (2 per probe) filtered post simulations

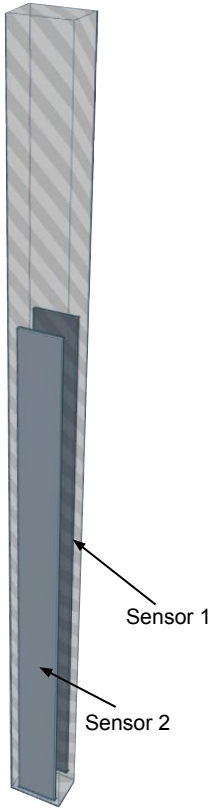

[1] *W. P. Segars, Molecular Imaging and Biology, 2004.*

Input - Source

Radiotracer: **[^{11}C]Raclopride**

- ^{11}Carbon radiolabeled **dopamine D2 receptor antagonist**[1,2]
- Preclinical/clinical research **schizophrenia**, **addictions**
- **Uptake in Harderian glands** (potential source of noise)
- Mean **range** of ^{11}C positrons ≈ **1.1 mm** (> ^{18}F ≈ 0.6 mm)

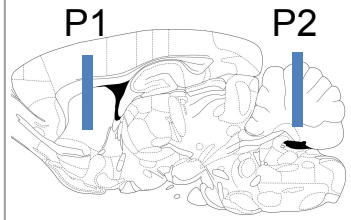

Striatum: **Specific signal**

Cerebellum: **Reference tissue**
→Free radioligand concentration: nonspecific **binding in the brain**

[1] *H. Hall et al, Prog Neuropsychopharmacol Biol Psychiatry. 1988*
[2] *N. Ginovart et al, Mol Imaging Biol*, 2005

Input - Source

Radiotracer: [^{11}C]Raclopride

Simplified Reference Tissue Model (SRTM)[3]:

$$C_{Model}(t) = R_1\, C_T'(t) + \left[k_2 - R_1\, k_2 / \left(1 + BP_{ND}\right)\right] C_T'(t) \otimes e^{-k_2 t/(1+BP_{ND})}$$

- ^{11}Carbon radiolabeled **dopamine D2 receptor antagonist**[1,2]
- Preclinical/clinical research **schizophrenia**, **addictions**
- **Uptake in Harderian glands** (potential source of noise)
- Mean **range** of ^{11}C positrons ≈ **1.1 mm** (> ^{18}F ≈ 0.6 mm)

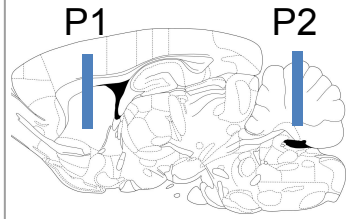

Striatum: **Specific signal**

Cerebellum: **Reference tissue**
→Free radioligand concentration: nonspecific **binding in the brain**

- [^{11}C]Raclopride time activity curves of **anesthetized rat**

  →9 MBq injection, dynamic **micro-PET** acquisitions
  (CERMEP, Biomaps-SHFJ)

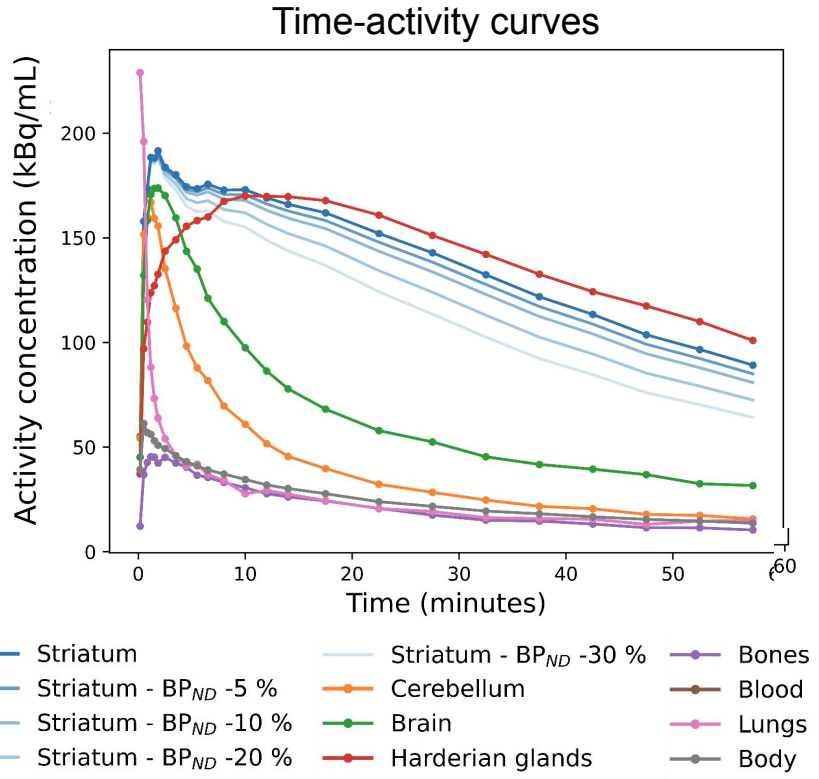

[1] *H. Hall et al, Prog Neuropsychopharmacol Biol Psychiatry. 1988*
[2] *N. Ginovart et al, Mol Imaging Biol*, 2005
[3] *A. Lammertsma & S. P. HUME, NEUROIMAGE 1996*

Results - Organ/particle contributions

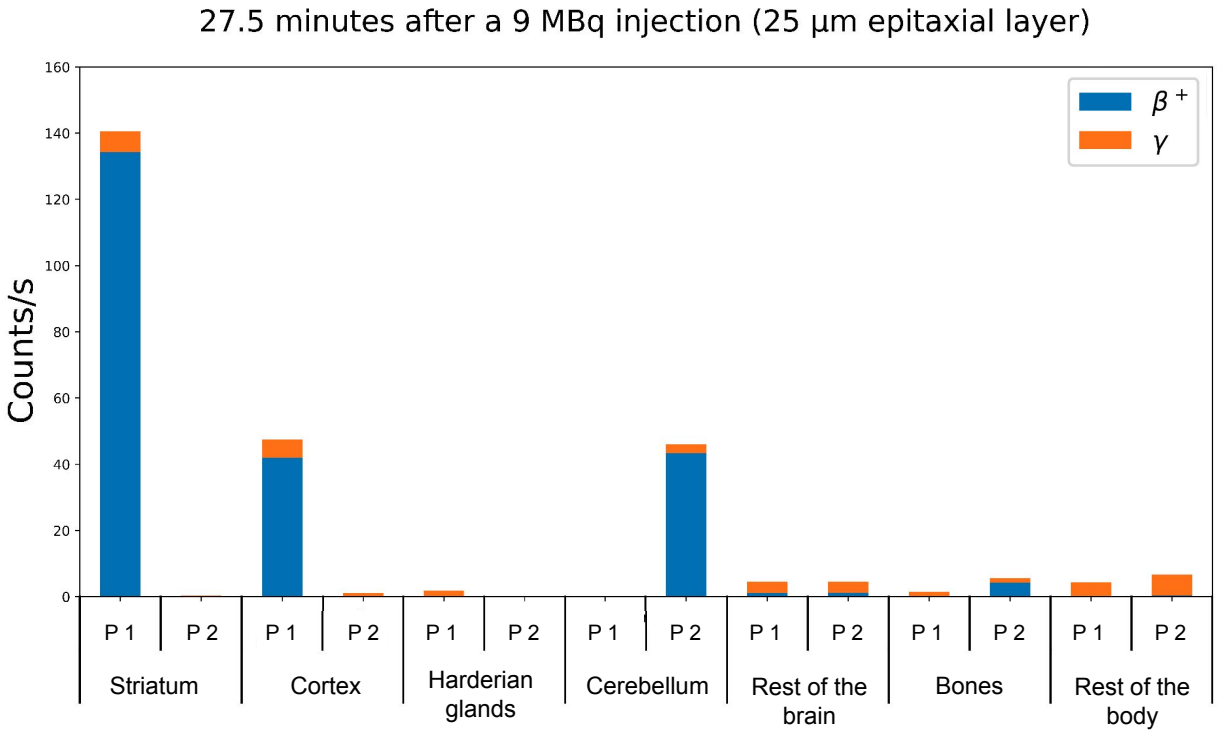

P1 = Striatum area P2 = Cerebellum area

Emission of detected particles:

→> 99% of detected particles from **skull area**

→Count rate:
≈ 265 ± 0.2 cps (25 µm)

→High **direct sensitivity**
≈ 89% of events in probe 1 (25 µm)

→Low **gamma sensitivity**

→Harderian glands signal **< 1%**

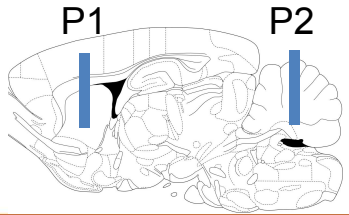

Results - Organ/particle contributions

Source position of detected particles:

→ **Local information**: more than **93%** of detected particles emitted within the first **2 mm surrounding** the probe 1

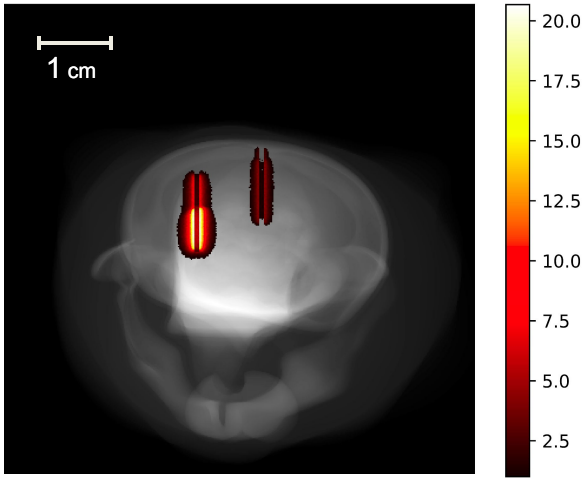

Coronal

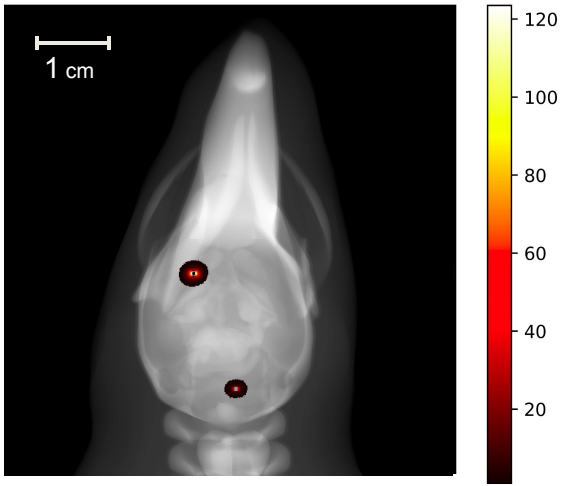

Axial

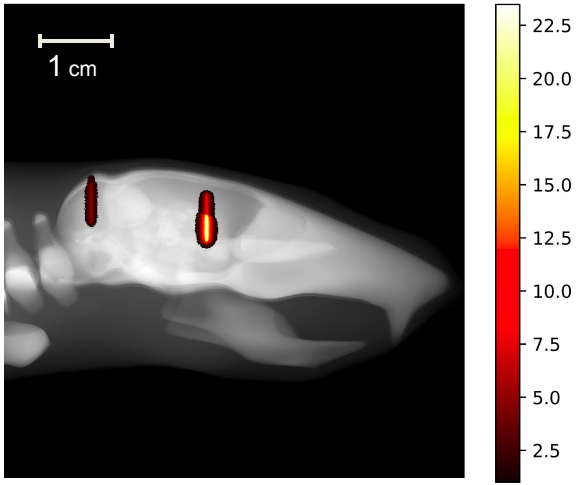

Sagittal

Integration over 1 minute, 27 minutes after injection (25 µm sensitive layer)

Results - Kinetic study

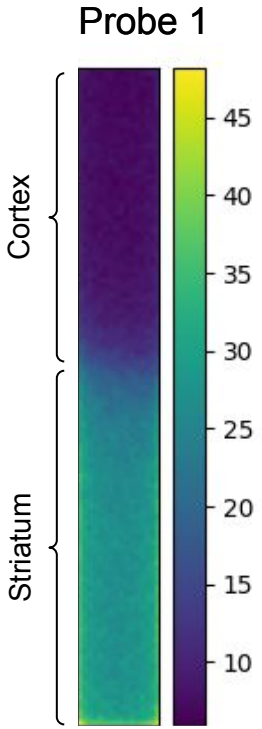

Probe 1 integrated image over 1 minute (striatum + cortex)

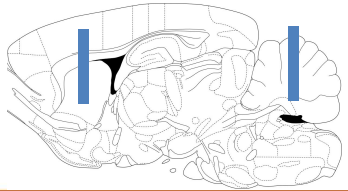

Results - Kinetic study

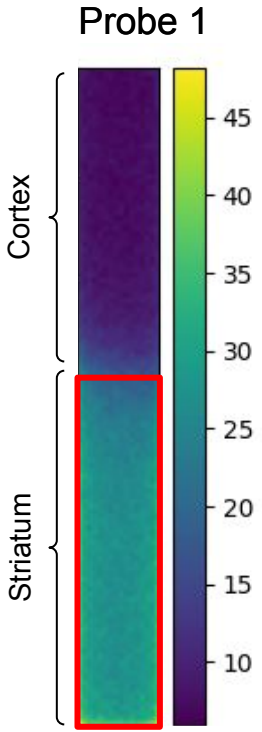

Probe 1 integrated image over 1 minute (striatum + cortex)

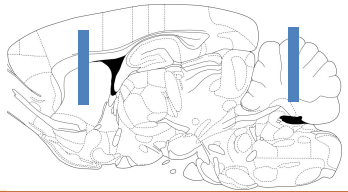

Results - Kinetic study

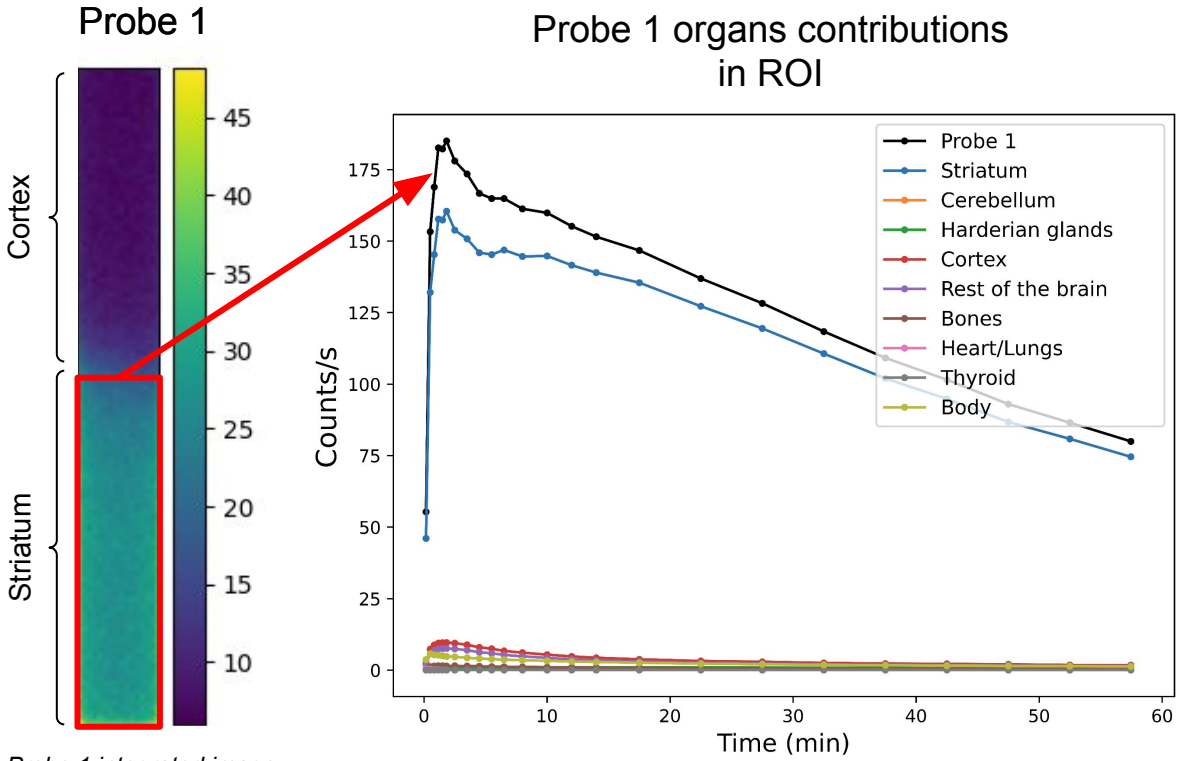

Probe 1 integrated image over 1 minute (striatum + cortex)

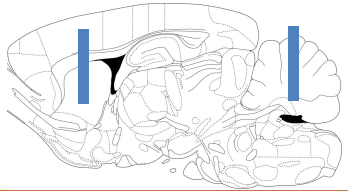

Results - Kinetic study

Probe 1

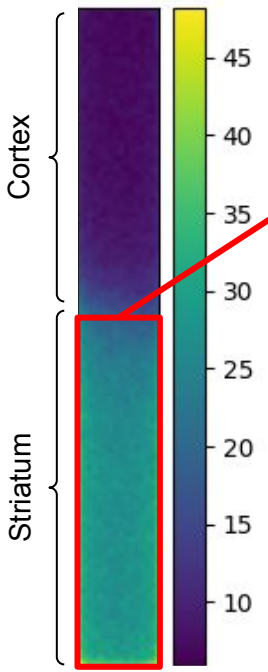

Probe 1 integrated image over 1 minute (striatum + cortex)

Probe 1 organs contributions in ROI

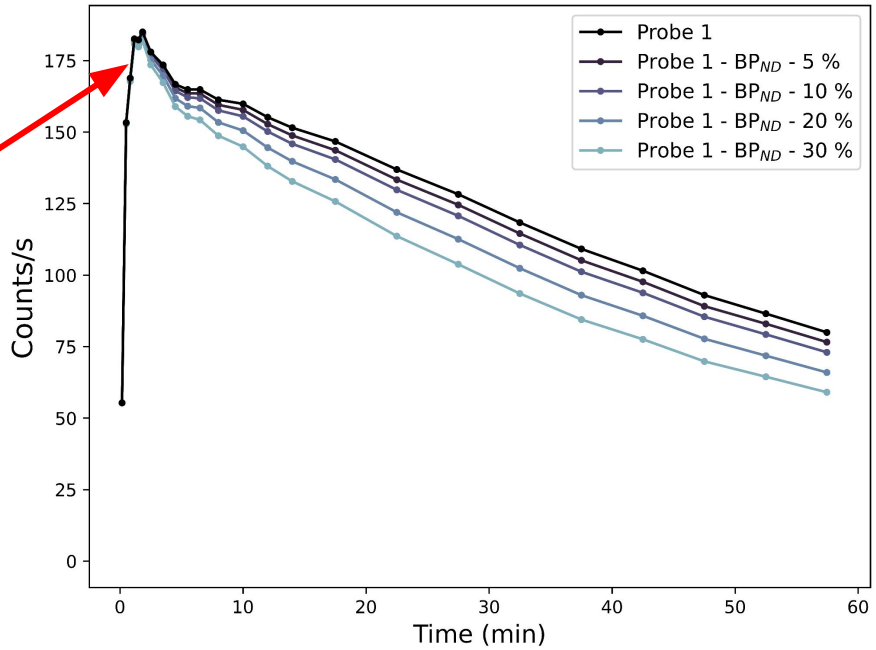

Simplified Reference Tissue Model (SRTM):

$$C_{Model}(t) = R_1 C_T'(t) + \left[k_2 - R_1 k_2 / \left(1 + BP_{ND}\right)\right] C_T'(t) \otimes e^{-k_2 t / (1 + BP_{ND})}$$

Results - Kinetic study

Probe 1

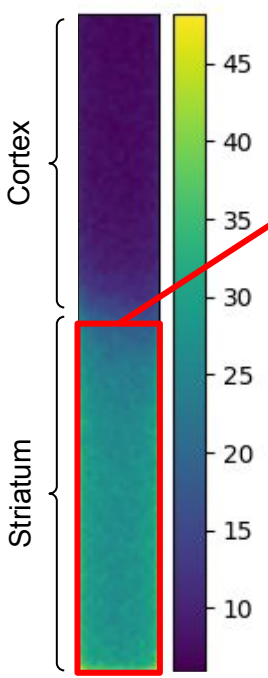

Probe 1 integrated image over 1 minute (striatum + cortex)

Probe 1 organs contributions in ROI

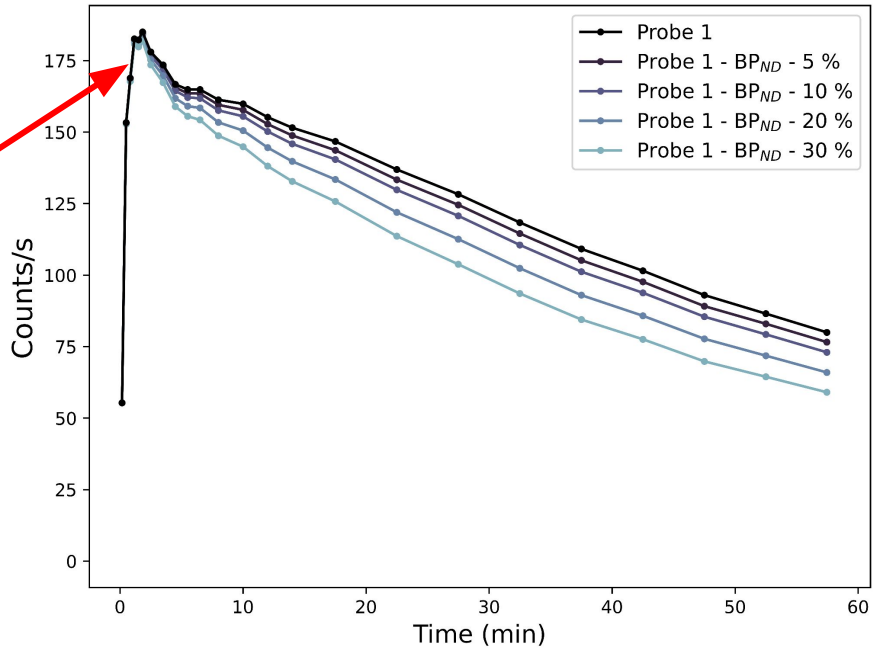

Simplified Reference Tissue Model (SRTM):

$$C_{Model}(t) = R_1 C_T'(t) + \left[k_2 - R_1 k_2 / \left(1 + BP_{ND}\right)\right] C_T'(t) \otimes e^{-k_2 t / (1 + BP_{ND})}$$

Input BP_{ND} variation	Measured BP_{ND} variation	Error on BP_{ND} variation
- 5 %	- 4.81 %	- 3.8 %
- 10 %	- 9.65 %	- 3.5 %
- 20 %	- 19.38 %	- 3.1 %
- 30 %	- 29,19 %	- 2.7 %

Quantification of the Binding potential (BP_{ND}) variations **consistent with the input BP_{ND}** variations.

Summary

Conclusion

- **New implantable β^+ microprobe produced**
- Performances in line with the **intended application**
  - High **β^+ sensitivity**
  - Low **γ sensitivity**

  } → **Local radiotracer uptake**
- Ability to quantify **variations of kinetic parameters**

Summary

Conclusion

- **New implantable β^+ microprobe produced**
- Performances in line with the **intended application**
  - High **β^+ sensitivity**
  - Low **γ sensitivity**

  } → **Local radiotracer uptake**
- Ability to quantify **variations of kinetic parameters**

Perspectives

- **Probe physical validation**
- **Biological validation** aimed for early 2024
  - Comparison MAPSSIC / micro-PET
- **Behavioral applications** aimed for early 2025

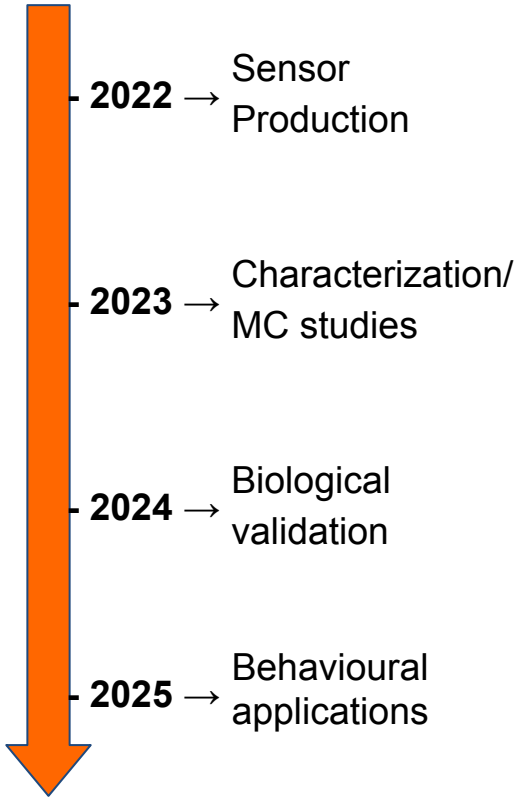

Acknowledgments

THANKS FOR YOUR ATTENTION

MAPSSIC Collaboration

Franck Agnese
Luis Ammour
Jérôme Baudot
Caroline Bouillot
Sandrine Bouvard
Olivier Clausse
Mathieu Dupont
Samir El ketara
Fabrice Gensolen
Maciek Kachel
Philippe Lanièce
Jérôme Laurence
Christian Morel
Patrick Pangaud
Marc-Antoine Verdier
Christophe Wabnitz
Téo Weicherding
Luc Zimmer

With financial support from MITI (Mission pour les initiatives transverses et interdisciplinaires du CNRS)

Affinity propagation algorithm

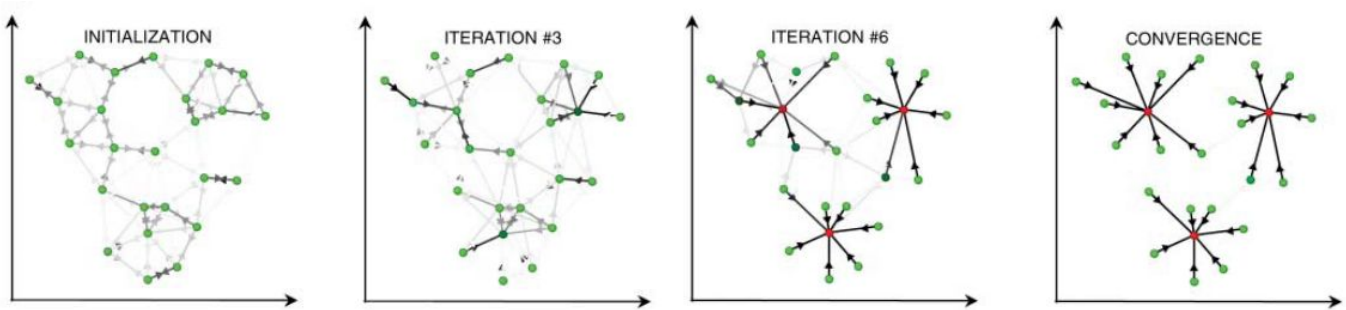

Brendan J. Frey and Delbert Dueck, "Clustering by Passing Messages Between Data Points", Science Feb. 2007

- Influence parameter :
  - ***Preference*** : Calculated number of clusters is **directly influenced** by the *preference* value

→Need for **calibration** of the algorithm : Search for the optimal *preference* value for AP clustering on frames containing from 1 to 100 clusters

Data generation

Affinity propagation algorithm - Calibration

Data processing from AP calibration runs:

- Determination of the optimal *preference*:
  - AP runs on calibration frames **scanning** the previously determined ***preference* range**
  - **Mean** and **Mode** of the distribution *preference* values leading to the **smallest error** between calculated and actual cluster number for a given frame
  - Gaussian draw of a new *preference* value if the previous does not converge to an answer (400 times maximum)

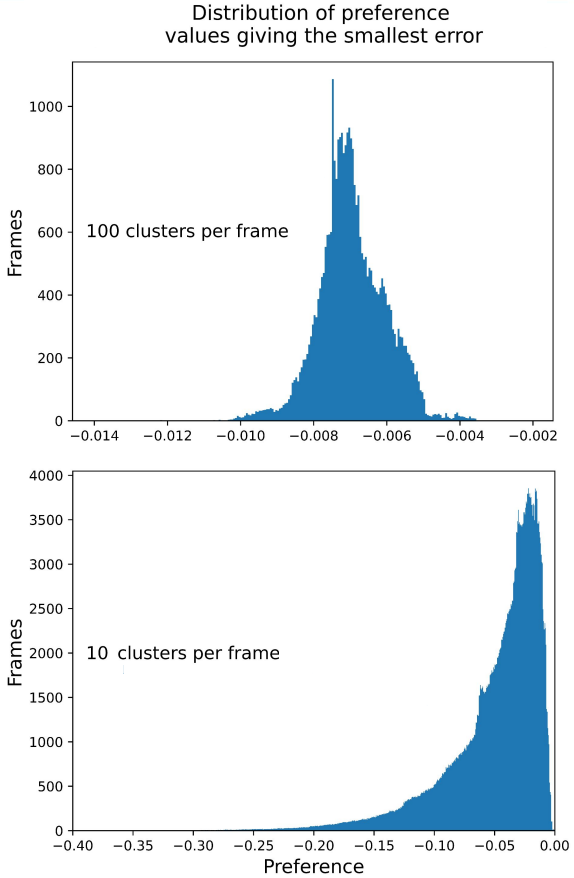

Data treatment

Raw Frame	Events
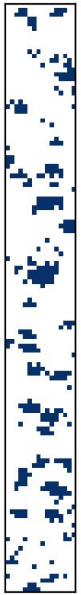	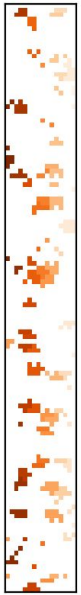

- Calibration of a machine learning algorithm (Affinity propagation algorithm)
- Application on **experimental Data** from ^{18}F radioactive decay measurement (IMIC-V1):

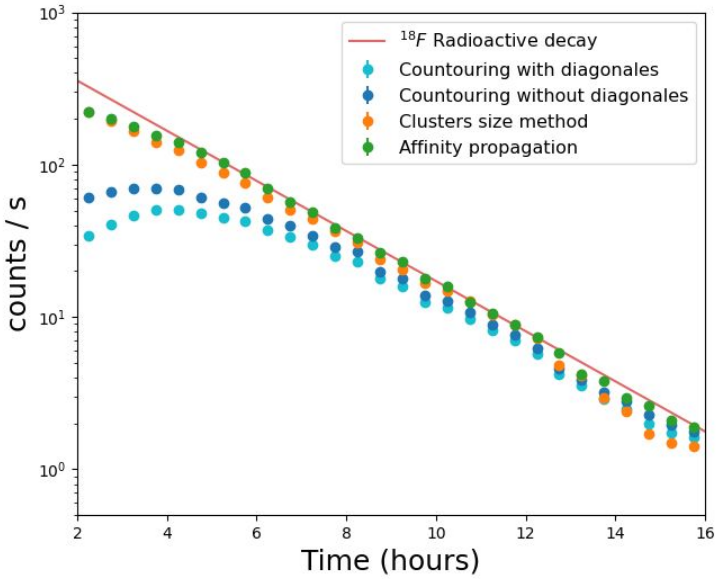

- **Achieved linearity** for the expected count rates for in vivo measurements
- Calculation time varies from **few milliseconds** to 0.5 seconds per frame
- **Spatial error** < 50 µm

Results compatible with *in vivo* measurements

Affinity propagation algorithm - Spatial performances

Spatial study : Error on cluster barycenter

- **Errors** on x and y axis: mean σ of **16.5 µm** and **26.2 µm**
  → 95% error equal or smaller than pixels size (2σ)
- Error (≈ µm) **<** explored structures (ie: rat striatum ≈ mm)

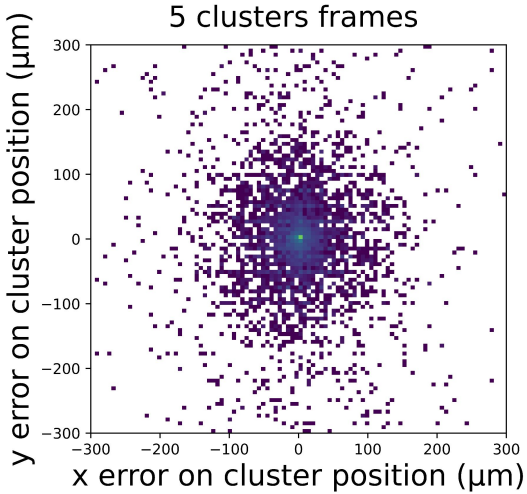

σ_x = 23.9 µm σ_y = 88.9 µm

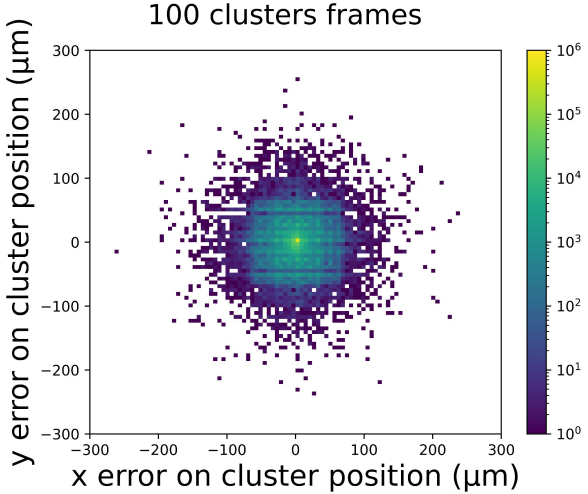

σ_x = 15.5 µm σ_y = 17.5 µm

Results - Kinetic study

Probe 1

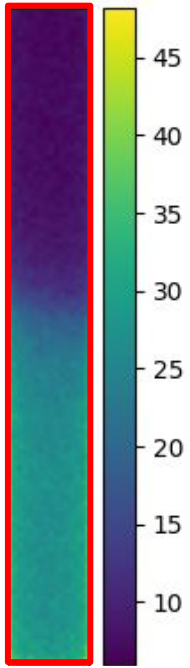

Probe 1 integrated image over 1 minute

Probe 1 organs contributions

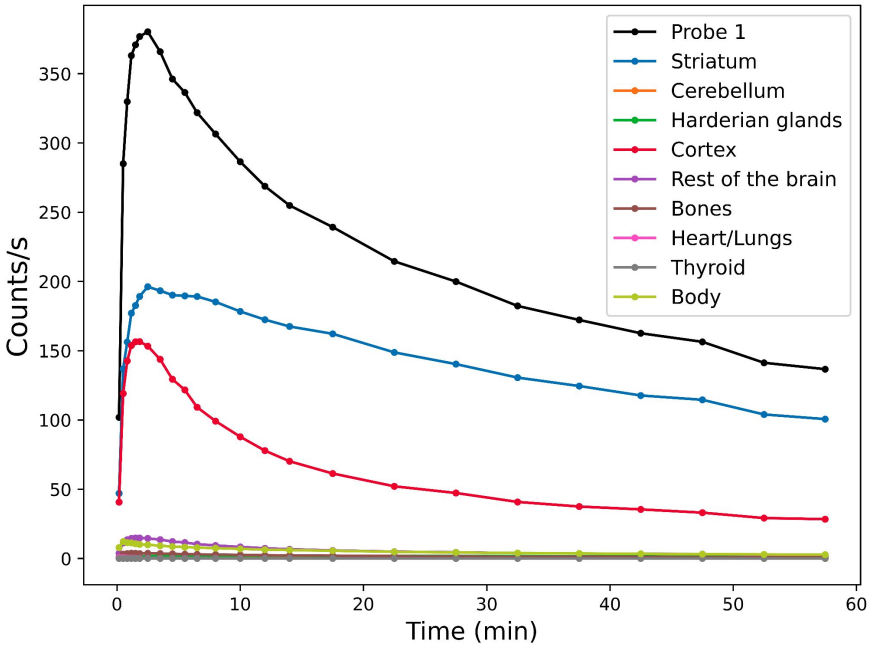

Striata signal in ROI vs overall striata signal in frame	Other organs contributions in ROI
100 %	30 %

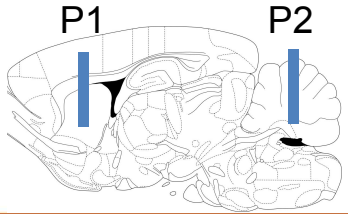

Results

Probe 1

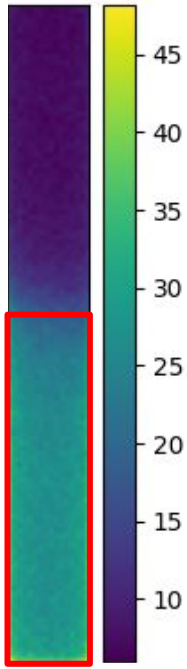

Probe 1 integrated image over 1 minute (striatum + cortex)

Probe 1 organs contributions in ROI

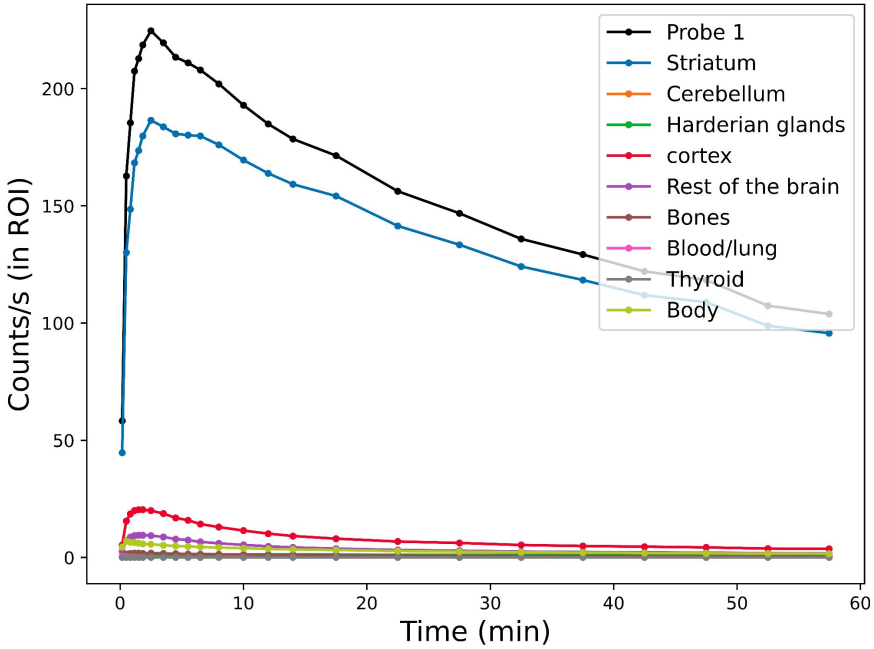

Striata signal in ROI vs overall striata signal in frame	Other organs contributions in ROI
> 95 %	< 8 %

- Next steps:
  - **kinetic modeling** with a compartmental model
  - Next step: input data from **awake animals**

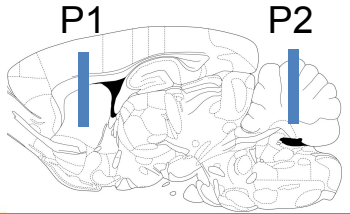

Input - Source

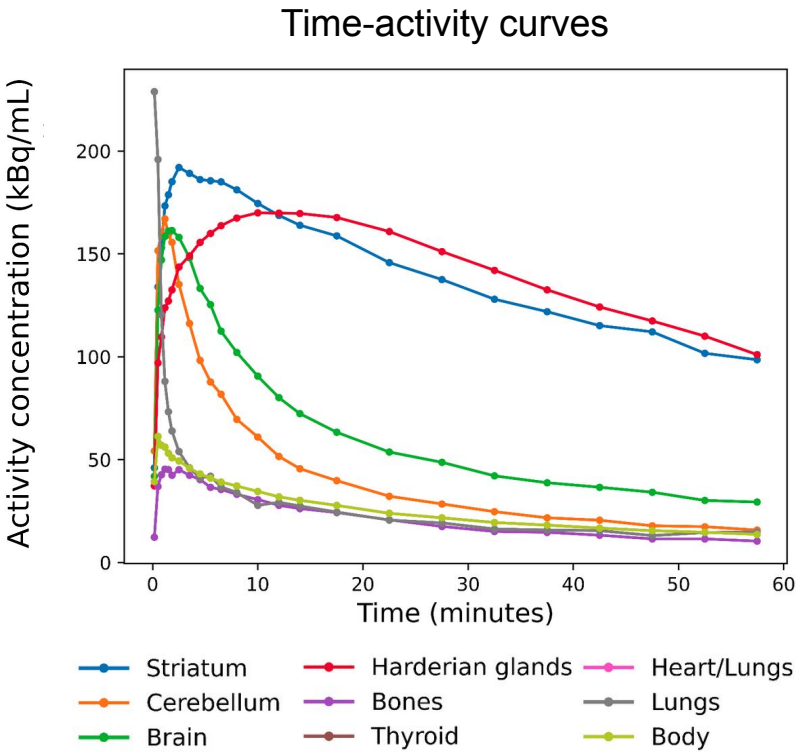

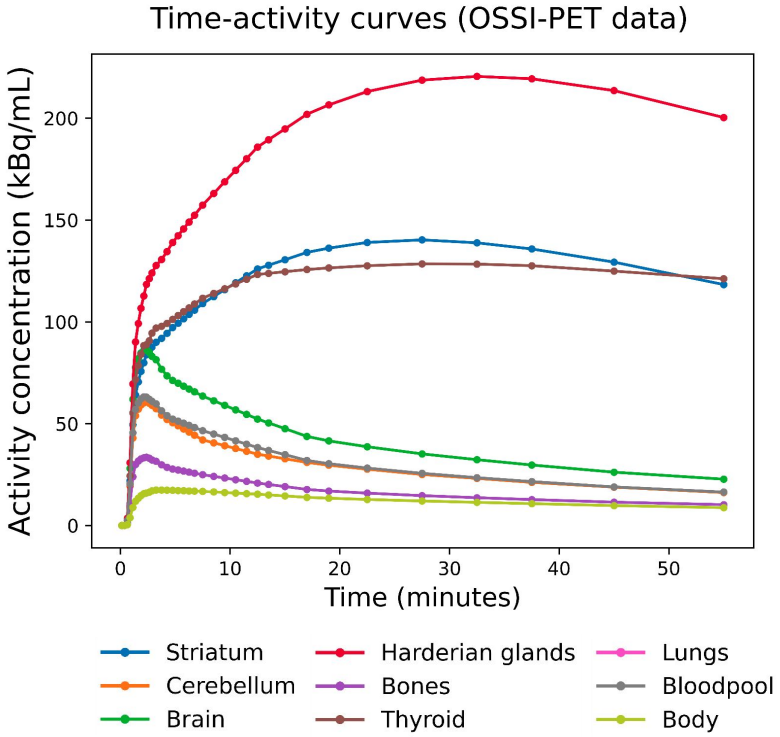

Results - Kinetic study

Input BP_{ND}	Measured BP_{ND}	Error on BP_{ND}	BP_{ND} variation	Measured BP_{ND} variation
3.0941	2.3919	22.7 %	0	-
2.9394	2.2769	22.5 %	- 5	- 4.81 %
2.7847	2.1611	22.4 %	- 10	- 9.65 %
2.6300	2.0442	22.3 %	- 15	- 14.54 %
2.4753	1.9283	22.1 %	- 20	- 19.38 %
2.3206	1.8109	22.0 %	- 25	- 24.29 %
2.1659	1.6936	21.8 %	- 30	- 29.19 %